Tree Physiology 31, 727–739
doi:10.1093/treephys/tpr064

Research paper

How does P affect photosynthesis and metabolite profiles of *Eucalyptus globulus*?

Charles R. Warren[1]

School of Biological Sciences, Heydon-Laurence Building A08, University of Sydney, Sydney, NSW 2006, Australia; [1]Corresponding author (charles.warren@sydney.edu.au)

Received February 28, 2011; accepted June 1, 2011; handling Editor Torgny Näsholm

Phosphorus (P) has multiple effects on plant metabolism, but there are many unresolved questions especially for evergreen trees. For example, we do not know the general effects of P on metabolism, or if P affects photosynthesis via the internal conductance to CO_2 transfer from sub-stomatal cavities to chloroplast or amounts of Rubisco. This study investigates how P deficiency affects seedlings of the evergreen tree *Eucalyptus globulus* grown for 2.5 months with four nutrient solutions differing in P concentration. To determine why photosynthesis was affected by P supply, Rubisco was quantified by capillary electrophoresis, internal conductance was quantified from gas exchange and carbon isotope discrimination, and biochemical parameters of photosynthesis were estimated from A/C_c responses. Additional insights into the effect of P on metabolism were provided by gas chromatography-mass spectrometry (GC-MS) metabolite profiling. Larger concentrations of P in the nutrient solution led to significantly faster rates of photosynthesis. There was no evidence that stomatal or internal conductances contributed to the effect of P supply on photosynthesis. The increase in photosynthesis with P supply was correlated with V_{cmax}, and amounts of P, phosphate and fructose 6-phosphate (6-P). Phosphorous supply affected approximately one-third of the 90 aqueous metabolites quantified by GC-MS, but the effect size was generally smaller than reported for experiments on herbaceous species. Phosphorus deficiency decreased concentrations of phosphate, glucose 6-P and fructose 6-P more than it decreased photosynthesis, suggesting faster turnover of smaller pools of phosphate and phosphorylated intermediates. The effect of P supply on most amino acids was small, with the exception of arginine and glutamine, which increased dramatically under P deficiency. P deficiency had small or non-significant effects on carbohydrates and organic acids of the tricarboxylic acid (TCA) cycle. The small effect of P on carbohydrates, organic acids and (most) amino acids likely reflects a functional homeostasis among C metabolism (glycolysis, TCA and pentose P cycles), rates of photosynthesis and growth. The strong functional homeostasis in *E. globulus* may reflect a conservative, long-term growth and metabolic strategy of evergreen trees.

Keywords: C_c, GC-MS, internal conductance, mesophyll conductance, metabolism, metabolite, nutrition, transfer conductance.

Introduction

Phosphorus (P) plays a central role in almost all aspects of plant metabolism and is one of the nutrients that most commonly limits growth. Photosynthesis is commonly reduced by P deficiency (Kirschbaum and Tompkins 1990, Turnbull et al. 2007) because of the requirement for a finely balanced concentration of orthophosphate (P_i) in the cytosol (Walker and Robinson 1978). The clear limitation of photosynthesis by cytosolic P_i was demonstrated in *Eucalyptus globulus* by sequestering cytosolic P_i with mannose; when P_i was sequestered with mannose, A_{max} was reduced by 83% (Turnbull et al. 2007). Artificial manipulation of cytosolic P_i demonstrates how photosynthesis is affected by P deficiency in the short term (minutes to hours), but it is less clear how P affects photosynthesis at longer time scales (i.e., days to months). Analyses of A/C_i responses indicate that P limitation decreases the maximum rate of CO_2-limited carboxylation (V_{cmax}) and triose phosphate utilization (TPU) (Lewis et al. 1994), V_{cmax} and RuBP-regeneration-limited rates of electron

transport (J_{max}) (Loustau et al. 1999), or V_{cmax}, J_{max} and TPU (Niinemets et al. 1999). Hence, in the case of long-term P deficiency, P_i metabolism (as indicated by the TPU parameter) is not the only limitation of photosynthesis—there may also be limitations in RuBP regeneration (as indicated by J_{max}) and/or the amount or activity of Rubisco (as indicated by V_{cmax}). One explanation for an effect of P on V_{cmax} is that there may be a strong positive correlation between P supply and the relative and absolute amounts of Rubisco (Warren and Adams 2002).

Relationships between P and photosynthesis can also arise if P supply affects the resistance to CO_2 movement from atmosphere to chloroplasts. For example, some studies have suggested that P-limited plants have slower photosynthesis compared with P-replete controls due to reduced stomatal conductance and concentrations of CO_2 in sub-stomatal cavities (C_i) (e.g., Kirschbaum and Tompkins 1990, Lewis et al. 1994). However, stomatal conductance is only part of the pathway from atmosphere to chloroplasts. The resistance to CO_2 movement from sub-stomatal cavities to chloroplasts (as described by internal conductance, g_i) reduces the CO_2 concentration in the chloroplasts (C_c) of most species by 60–90 μmol mol^{-1} below C_i (see review data in Warren 2008). One consequence of the large and variable drawdown from C_i to C_c is that to disentangle the effects of P on biochemistry from effects on CO_2 diffusion requires knowledge of C_c. With only one exception (Bown et al. 2009), previous studies of P and photosynthesis have used C_i to imply diffusional limitations, and thus the derived 'biochemical' parameters (V_{cmax}, J_{max} and TPU) are not purely biochemical but also include information pertaining to C_i–C_c. In the only paper to investigate whether $C_i - C_c$ (or g_i) plays a role in photosynthesis under P limitation, the authors found that in *Pinus radiata* there was no effect of P supply on C_i– C_c or relative limitations due to g_i (Bown et al. 2009). Despite this negative result there is reasonable a priori basis for expecting P to affect g_i given that g_i is correlated with leaf anatomical and morphological traits (Terashima et al. 2006) that are commonly affected by P supply (Feller 1996, Sardans et al. 2006).

In addition to uncertainties regarding how P affects photosynthesis in any species, for evergreen trees we have only a rudimentary knowledge of how P affects other aspects of metabolism. In recent years there has been widespread use of metabolite profiling by gas chromatography-mass spectrometry (GC-MS) to examine how metabolism is affected by deficiencies of nitrogen (N) (Okazaki et al. 2008, Tschoep et al. 2009, Kusano et al. 2011) and P (Hernandez et al. 2007, Huang et al. 2008). These past studies focused on species such as *Arabidopsis*, rice, common bean and cereals and have indicated widespread effects of P deficiency on multiple classes of metabolites (e.g., amino acids, tricarboxylic acid (TCA) cycle organic acids, carbohydrates, phenylpropanoids) (Pieters et al. 2001, Nanamori et al. 2004, Hernandez et al. 2007, Huang et al. 2008). In contrast, little is known about how P deficiency affects metabolites in evergreen trees such as those from the genus *Eucalyptus*. The foliage of evergreens serves dual roles of photosynthesis and nutrient storage (Chabot and Hicks 1982, Vapaavuori et al. 1995, Millard 1996), and thus herbaceous species are uncertain models for evergreen trees with respect to nutrition and photosynthesis (Warren and Adams 2004*b*). This study investigates how P deficiency affects seedlings of *E. globulus*. *Eucalyptus globulus* is the most common plantation *Eucalyptus* species in temperate regions and almost completed sequencing means *Eucalyptus* is set to become the second model tree genus for functional genomics (after *Populus*). Metabolite profiling by GC-MS was used to examine responses of metabolites to P supply. To determine why photosynthesis is affected by P supply, internal conductance was quantified from simultaneous measurements of gas exchange and carbon isotope discrimination (Evans et al. 1986) and used to calculate C_c, which was then used to parameterize a biochemical model of C3 photosynthesis (Farquhar et al. 1980). The stable carbon isotope composition of leaves was determined to obtain a measure of C_c integrated over the time that carbon in the leaf was fixed (Farquhar et al. 1989).

Materials and methods

Plant growth and experimental design

Seed of *E. globulus* ssp. *globulus* (CSIRO ATSC seedlot 18725) was obtained from the Australian Tree Seed Centre (Kingston, ACT, Australia). Seed was germinated in moist vermiculite in a sunlit polythene-covered greenhouse that transmitted around 70% of sunlight. Germinants were carefully transferred to 2 l plastic pots filled with perlite and for the first month after transfer to pots were irrigated to field capacity three times per week with a balanced nutrient solution at one-quarter of its normal concentration. The nutrient solution was modified from a formulation used in several previous experiments with seedlings of *E. globulus* and other *Eucalyptus* species (e.g., Turnbull et al. 2007). Perlite was used as the growth medium because its ion exchange capacity buffered P concentrations in the soil solution against rapid fluctuations (e.g., due to addition of nutrients and watering).

Twenty seedlings were randomly assigned to one of four P treatments (0.1, 0.02, 0.005 and 0.0 mM P, as equimolar K_2HPO_4 and KH_2PO_4). These P concentrations were chosen based on a pilot experiment with *E. globulus* in perlite substrate, and past experience with the same species growing with a sand substrate. The pilot study indicated that to produce an adequate range in P availability (as indicated by foliage N:P), the P concentration of the nutrient solution had to be decreased 3.5-fold compared with previous studies using a sand substrate (e.g., Turnbull et al. 2007). In addition to the nominated P concentration, nutrient solutions contained 6 mM N (as 3 mM NH_4NO_3), 4 mM K, 2.9 mM Ca, 1.5 mM Mg, 1.5 mM S,

52 μM Mn, 49 μM Fe, 20 μM Cu, 15 μM Zn, 8 μM B and 0.03 μM Mo. P was supplied as potassium phosphate and thus differing amounts of K were supplied with the different P treatments; however, it was not necessary to compensate for the additional K because it led to a <4% deviation from the nominated K concentration. For 2.5 months seedlings were irrigated to field capacity with nutrient solution four times per week, and with water on the remaining days. The 2.5-month duration of the experiment was sufficiently long for new leaves to be produced in all treatments, but sufficiently short to avoid significant root binding. The mean temperature inside the greenhouse during the period of nutrient treatments were imposed (February to April 2009) was 22.1 °C with an absolute maximum of 35.8 °C and a minimum of 11.7 °C. Average daily photosynthetically active radiation (PAR) inside the greenhouse was 472 μmol m^{-2} s^{-1} (18.8 mol m^{-2} day^{-1}) with an absolute maximum of 1601 μmol m^{-2} s^{-1}. Daily maximum and minimum temperatures and maximum PAR are given as supplementary information available as Supplementary Data at *Tree Physiology* Online.

Simultaneous measurement of gas exchange and carbon isotope discrimination

After P treatments had been imposed for 2.5 months, gas exchange parameters were measured on each of five replicate plants per treatment using a LI-6400 system (LI-Cor, Lincoln, NE, USA) coupled to a tuneable diode laser (TGA100a, Campbell Scientific, Logan, UT, USA), essentially as described previously (Barbour et al. 2007). Rather than the standard LI-Cor 6 cm^2 chamber, a custom-built 18 cm^2 chamber illuminated by a LED light source (LI6400-18 RGB) was used. The larger chamber was necessary to enable a sufficiently large drawdown in chamber CO_2 for reliable measurements of internal conductance. Precision of measurement of $\delta^{13}C$ was routinely better than 0.06‰ (sd, $n = 10$).

All measurements were made on the youngest fully expanded leaf that had developed under the nutrient treatments. A leaf was enclosed in the chamber and acclimated at a CO_2 concentration of 400 μmol mol^{-1} ($\delta^{13}C = -5$ to -6.5‰), a temperature of 25 °C, a light-saturating PAR of 2000 μmol m^{-2} s^{-1} and a leaf-to-air vapour pressure deficit of 0.8–1.3 kPa. Molar flow of air through the gas exchange chamber was varied among leaves between 250 and 500 μmol s^{-1}, depending on rates of gas exchange. Once rates of photosynthesis and transpiration were steady, gas exchange parameters were recorded every 30 s for 18–25 min. Every 180 s, the tuneable diode laser recorded a 30-s average of $^{13}CO_2$ and $^{12}CO_2$ of air entering and leaving the gas exchange chamber. Carbon isotope data were not corrected for diffusion of CO_2 into and out of the leaf chamber because this was insignificant (<0.01‰) due to the small difference in CO_2 concentration and $\delta^{13}C$ between air in the gas exchange system (300–400 μmol mol^{-1}, $\delta^{13}C = -5$ to -6.5‰) and ambient air in the greenhouse (350–450 μmol mol^{-1}, $\delta^{13}C = -8$ to -10‰).

Carbon isotope discrimination by the shoot (Δ_{obs}) was calculated as described previously (Evans et al. 1986):

$$\Delta_{obs} = \xi(\delta_o - \delta_e)/(1 + \delta_o - \xi[\delta_o - \delta_e]), \quad (1)$$

where δ_o and δ_e are the carbon isotope composition ($^{13}C/^{12}C$) of air entering (δ_e) or leaving (δ_o) the chamber. Carbon isotope composition was expressed against the carbon isotopic composition of the Pee Dee Belemnite (PDB) formation, where $\delta = 1000\ [(({}^{13}C_{sample}/{}^{12}C_{sample})/({}^{13}C_{PDB}/{}^{12}C_{PDB})) - 1]$. $\xi = uC_e/(sA)$ where u is the molar flow rate through the chamber, C_e is the concentration of CO_2 entering the chamber, A is the rate of photosynthesis and s is the projected leaf area. g_i was estimated from the difference between calculated carbon isotope discrimination assuming infinite g_i (Δ_i), and that measured by the coupled system (Δ_{obs}, Evans et al. 1986):

$$\Delta_i = a_b \frac{C_a - C_s}{C_a} + a\frac{C_s - C_i}{C_a} + b\frac{C_i}{C_a} - f\frac{\Gamma^*}{C_a} - e'\frac{R_d}{A + R_d}\frac{C_i - \Gamma^*}{C_a} \quad (2)$$

and

$$g_i = \frac{A(b - a_i - b_s - (e'R_d/A + R_d))}{C_a(\Delta_i - \Delta_{obs})} \quad (3)$$

where Δ_i is the expected carbon isotope discrimination when g_i is infinite, C_a is the CO_2 concentration in ambient air, C_s is the CO_2 concentration at the leaf surface, C_i is the CO_2 concentration in the sub-stomatal cavity (calculated after accounting for mean epidermal conductance of 6.5 mmol m^{-2} s^{-1}), a_b is the carbon isotope discrimination during diffusion through the boundary layer (2.9‰), a is the carbon isotope discrimination during diffusion through stomata (4.4‰) a_i is the carbon isotope discrimination during CO_2 diffusion in water (0.7‰), b is the carbon isotope discrimination caused by Rubisco and phosphoenol pyruvate carboxylase (30‰), b_s is the fractionation as CO_2 enters solution (1.1‰), f is the carbon isotope discrimination due to photorespiration (11.6‰, Lanigan et al. 2009), Γ^* is the CO_2 compensation point in the absence of dark respiration (43 μmol mol^{-1} at 25 °C in multiple *Eucalyptus* spp., C. Warren unpublished data) and e' is the combined carbon isotope discrimination due to dark respiration (–3‰, Bickford et al. 2009) and the ^{13}C disequilibrium between growth and measurement CO_2 (Wingate et al. 2007, Tazoe et al. 2009). e' was calculated for each measurement and varied between –2 and –0.5‰ due to variation in $\delta^{13}C$ of reference gas. g_i was calculated from (2) and (3) for each measurement and a mean was calculated for the 18–25 min each leaf was measured.

Measurement of the CO_2 response of photosynthesis

After P treatments had been imposed for 2.5 months, the CO_2 response of photosynthesis was determined with a 2 × 3 cm

broadleaf chamber with an integrated light source (LI-6400-02B, LI-Cor). Measurements were made at 25 °C and a leaf-to-air vapour pressure deficit of 0.8–1.3 kPa. The molar flow rate through the chamber was 400 μmol s^{-1}. Leaves were exposed to 400 μmol mol^{-1} CO_2 in air and a photosynthetic photon flux density of 2000 μmol m^{-2} s^{-1} until the rates of photosynthesis and transpiration were steady (typically 20–30 min). After this, C_a was increased to 2000 μmol mol^{-1} and an $A - C_i$ curve was generated by decreasing C_a to 50 μmol mol^{-1} in 10 steps. At each C_a, photosynthesis was allowed to stabilize for at least 3 min. V_{cmax}, J and TPU were determined from measured A and C_c (calculated as $C_c = C_i - A/g_i$, assuming g_i is unaffected by [CO_2]) fitted to the photosynthesis model of Farquhar et al. (1980) with C_c-based kinetic constants (Bernacchi et al. 2002).

Plant harvest and measurement of P, N and $\delta^{13}C$

Plants were harvested 1 day after gas exchange measurements. From each plant two leaves were sampled between noon and 1 p.m. to control for possible diurnal variation in metabolites. The leaves sampled were youngest fully expanded leaves that had developed under the different nutrient treatments. One leaf was used for measuring P, N, stable carbon isotope composition ($\delta^{13}C$), metabolites and inorganic ions, while the other was used for measuring Rubisco. Both samples were immediately frozen in liquid N and stored at –80 °C. After leaves had been sampled, plants were divided into root, stem and leaves and stored at –80 °C. P, N and $\delta^{13}C$ of leaf, stem and root samples were determined on material that was freeze dried and then ground to a fine powder with a bead mill (30 s at 25 Hz with a 5 mm stainless steel bead) (TissueLyser, Qiagen, Doncaster, VIC, Australia). Phosphorus was determined using the colorimetric method of Murphy and Riley (1962) after digesting samples with HNO_3 and H_2O_2. The stable carbon isotope composition and nitrogen content were determined by isotope ratio mass spectrometry at the UC Davis Stable Isotope Facility.

Analysis of metabolites by GC-MS

Metabolites were extracted from freeze-dried leaves with methanol:chloroform:water and analysed by three GC-MS methods as described previously (Warren et al. 2011). The aqueous fraction of leaf extracts was analysed by GC-MS with three methods: methoximated trimethyl-silyl (TMS) derivatives with splitless injection and a slow temperature ramp, methoximated TMS derivatives with split injection and a faster temperature ramp, and *tert*-butyldimethyl-silyl derivatives used to quantify amino acids. Two separate injections of TMS derivatives were necessary because metabolite concentrations spanned more than five orders of magnitude, and thus the splitless method permitted identification of as many metabolites as possible but could not be used for quantification of abundant metabolites because they were well above the linear range of the mass spectrometer.

Methoximated TMS derivatives were prepared essentially as described previously (Lisec et al. 2006). For the splitless injection, 1 μl samples were injected into an injection port liner (single gooseneck Siltek-treated, Restek, Bellefonte, PA, USA) at 250 °C and separated on an arylene-modified 5% diphenyl–95% dimethyl polysiloxane stationary phase (30 m long × 0.25 mm inner diameter (i.d.) × 0.25 μm film thickness with a 10-m 'guard column'; Rxi-5SilMS, Restek). The column was held at 70 °C for 2 min, raised to 330 °C at 8 °C min^{-1}, and then held at 330 °C for 10 min. Helium (99.999%, BOC, North Ryde, NSW, Australia) was used as the carrier gas at a constant flow of 1 ml min^{-1}. The transfer line was held at 280 °C and the ion source at 250 °C. The column eluent was ionized by electron impact (70 eV) and mass spectra were collected from 70 to 600 amu at 6.67 scans per second (GCMS-QP2010Plus, Shimadzu, Kyoto, Japan). For the split injection, chromatographic conditions were similar except that 1 μl samples were injected with a 20:1 to 30:1 split into an injection port liner (FocusLiner™, SGE, Ringwood, VIC, Australia) at 275 °C, carrier gas flow was 1.5 ml min^{-1} and the column was held at 130 °C for 1 min, ramped to 330 °C at 15 °C min^{-1} and held at 330 °C for 6 min. Mass spectra were deconvoluted (AnalyzerPro, Spectralworks Ltd, Runcorn, UK) and metabolites were identified by comparing retention indices and mass spectra with a laboratory mass spectral/retention index library of 130 chemical standards (Warren et al. 2011). Criteria used in identification were retention index ±5 units and mass spectral match >75%. Mass spectra were also checked against the Golm Metabolome Database (Schauer et al. 2005), Agilent Fiehn GC/MS Metabolomics Library (Agilent, Santa Clara, CA, USA) and NIST05 Mass Spectral Library (National Institute of Standards and Technology, Gaithersburg, MD, USA). All chromatograms were checked by hand to remove deconvolution errors and mass spectral peaks due to contaminants (e.g., siloxanes). Metabolites matching 'unknowns' recorded in the GOLM database are reported using the Golm identifer. Metabolites that did match library or standards are identified and reported: EIMS_retention index.

Amino acids were quantified by GC-MS of *t*-BDMS derivatives, as described previously (Warren et al. 2011). Amino acids were identified based on retention indices and mass spectra of standards run under the same conditions: retention index within five units, reverse spectral match better than 80% and the ratio of quantification ion to two qualifier ions. Quantification was based on the dominant M-57 ions (ions with a mass 57 less than the intact molecular ion—corresponding to loss of a *t*-butyl group), with the exception of arginine, which was quantified based on the dominant M-188 ion (corresponding to loss of a *t*-butyl group plus a guanidino N).

Analysis of inorganic anions, inorganic cations and Rubisco by capillary electrophoresis

Inorganic anions and cations in the aqueous phase of leaf extracts were determined by capillary electrophoresis (CE) with indirect UV detection, as described previously (Warren and Adams 2004*a*). Rubisco was quantified by CE of sodium dodecyl sulphate–protein complexes (Warren et al. 2000). All CE separations used a commercial CE system with a UV-Vis detector (P/ACE MDQ, Beckman-Coulter Inc., Fullerton, CA, USA) and bare fused silica capillaries of 50 μm i.d.

Data analysis and statistics

Analyses of leaf metabolites were based on amounts per unit dry mass and per unit leaf area. Univariate statistics (analysis of variance (ANOVA)) were used to examine the effect of P on gas exchange. To perform multivariate statistics, data from the different analytical platforms were combined into a matrix. In cases where a metabolite had been measured on multiple analytical platforms, data from the most reliable platform were used (e.g., *t*-BDMS derivatives for amino acids, CE for phosphate). Multiple derivatives of the same metabolite were either averaged or the less reliable derivative was ignored. Metabolites present in <50% of samples of a treatment were omitted. Data were Pareto scaled and log transformed and then multivariate statistics were performed with SIMCA P+ (V 12.0.1, Umetrics, Umeå, Sweden). To separate predictive variation related to the P treatment from non-predictive (orthogonal) variation, orthogonal projection to latent structures discriminant analysis (OPLS-DA) was used with concentration of P in nutrient solution as the *y*-variable (Bylesjö et al. 2006). OPLS-DA was also used to investigate relationships between metabolites and A_{max} by using A_{max} as the *y*-variable. The significance of variables in OPLS-DA models was assessed as either VIP > 1, or loading ± confidence interval ≠ 0.

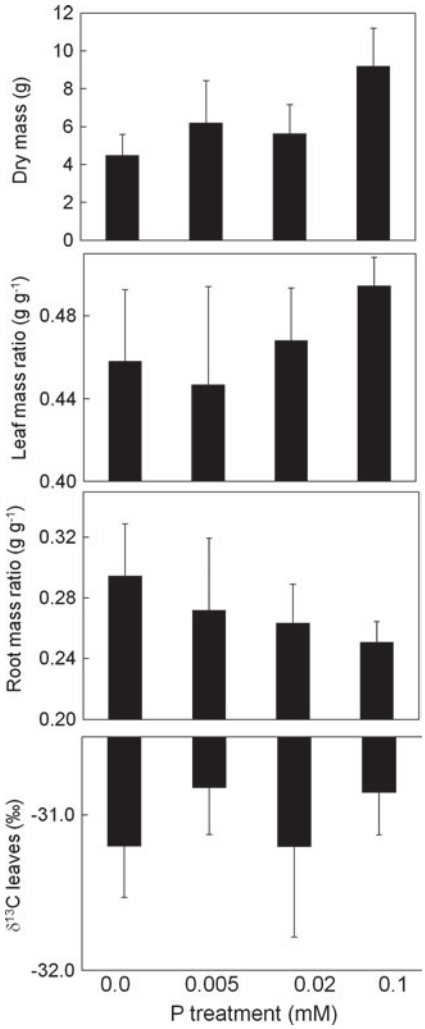

Figure 1. Dry mass, leaf and root mass ratio (leaf or root mass/total mass), and leaf carbon isotope ratio ($\delta^{13}C$) of *E. globulus* seedlings grown with one of four P treatments. Data are means of five replicates per treatment. Error bars are standard deviation.

Results

Dry mass, N and P

Specific leaf area (one-sided leaf area/dry mass) was 13 $m^2\ kg^{-1}$ and did not differ among treatments (data not shown). Phosphorus supply had a large effect on the growth of seedlings and concentrations of N and P (Figure 1 and Table 1). Dry mass in the P0.1 treatment was more than twice the dry mass in the 0.0 mM treatment (Figure 1). With increasing concentrations of P in the nutrient solution, there was a non-significant trend for decreased allocation to roots (root mass ratio, Figure 1) and increased allocation to leaves (leaf mass ratio, Figure 1). The stable carbon isotope composition of leaves ($\delta^{13}C$) did not differ among treatments (Figure 1), nor did the stable carbon isotope composition of stems or roots (data not shown). The P concentration of roots was larger in seedlings receiving higher concentrations of P in the nutrient solution, while the P concentration of stems was unaffected by P supply (data not shown). The P concentration of leaves was significantly higher in the P0.1 treatment (1.5 ± 0.2 mg g^{-1}, mean ± SD $n = 5$) compared with treatments with smaller P concentrations (Table 1). The N concentrations of roots and stem were higher in seedlings receiving higher concentrations of P in the nutrient solution (data not shown); however, in leaves the trend was for the highest concentration of N in P0.1 (19 ± 1 mg g^{-1}) followed by P0.0 (17 ± 1 mg g^{-1}) with the lowest concentration in P0.005 and P0.02 (15–16 mg g^{-1}). Nitrogen:phosphorus ratios in leaves were negatively related to P supply, decreasing from 26 g g^{-1} in the P0.0 treatment to 12 g g^{-1} in the P0.1 treatment. Rubisco content per unit area varied between 2.2 and 2.8 g m^{-2} and was unrelated to P treatment (Table 1). Rubisco N was 25–35% of total N and did not vary among treatments.

Table 1. Leaf chemistry and photosynthetic characteristics of seedlings of *E. globulus* grown with four different P treatments for 2.5 months. Data are N, P and Rubisco content per unit area. Gas exchange and tuneable diode laser measurements at ambient CO_2 and light-saturating PAR were used to determine the rate of net photosynthesis (A_{max}), stomatal conductance to water (g_s), sub-stomatal CO_2 concentration, internal conductance to CO_2 (g_i) and the drawdown in CO_2 from substomatal cavities to chloroplasts ($C_i - C_c$). Fits of A/C_i responses to a biochemical model of C3 photosynthesis were used to determine the maximum rate of carboxylation (V_{cmax}), electron transport (J) and triose phosphate utilization (TPU). Data are means (SD), $n = 5$ replicate plants. The significance of P treatment was determined by one-way ANOVA with probability indicated in the last row: * <0.05; ** <0.01; *** <0.001.

P treatment (mM)	N (mg m^{-2})	P (mg m^{-2})	N:P (g g^{-1})	Rubisco (mg m^{-2})	$\delta^{13}C$ (‰)	A_{max} (μmol m^{-2} s^{-1})	g_s (mol m^{-2} s^{-1})	C_i (μmol mol^{-1})	g_i (mol m^{-2} s^{-1})	$C_i - C_c$ (μmol mol^{-1})	V_{cmax} (μmol m^{-2} s^{-1})	J (μmol m^{-2} s^{-1})	TPU (μmol m^{-2} s^{-1})
0.0	1575 (122)	67 (23)	26 (10)	2.3 (1.0)	−31.2 (0.3)	8 (2)	0.18 (0.04)	291 (7)	0.15 (0.05)	61 (21)	49 (19)	84 (21)	6.9 (1.1)
0.005	1271 (96)	45 (12)	29 (6)	2.5 (0.5)	−30.8 (0.3)	11 (1)	0.21 (0.06)	274 (23)	0.20 (0.04)	55 (10)	51 (16)	87 (14)	6.9 (0.3)
0.02	1372 (135)	68 (7)	20 (3)	2.2 (1.0)	−31.2 (0.6)	11 (2)	0.30 (0.07)	300 (17)	0.17 (0.08)	74 (25)	55 (17)	90 (14)	7.2 (0.4)
0.1	1316 (83)	106 (12)	12 (2)	2.8 (1.6)	−30.8 (0.3)	13 (1)	0.27 (0.09)	267 (30)	0.25 (0.09)	57 (17)	83 (9)	152 (21)	12.1 (2.5)
P	**	***	**	NS	NS	**	NS	NS	NS	NS	*	***	***

Photosynthesis

A_{max} varied between treatment means of 8 and 13 μmol m^{-2} s^{-1}, g_s between 0.18 and 0.3 mol m^{-2} s^{-1}, and g_i between 0.15 and 0.25 mol m^{-2} s^{-1}. Higher concentrations of P in the nutrient solution led to significantly faster A_{max}. There were also increases in g_s and g_i, but these were statistically non-significant due to large variation between replicates. Neither C_i nor C_i–C_c was affected by P supply. V_{cmax}, J and TPU were approximately 50% higher in the P0.1 treatment than the three treatments with lower P concentrations. A_{max} was positively related to P content per unit area ($P = 0.045$, $R^2 = 0.24$, Figure 2) and Rubisco per unit area ($P = 0.044$, $R^2 = 0.34$, Figure 3), but was negatively related to N per unit area ($P = 0.040$, $R^2 = 0.25$). P per unit area was not related to g_s or g_i, while N per unit area was negatively related to g_s ($P = 0.025$, $R^2 = 0.29$) and unrelated to g_i (Figure 2).

Metabolite profile of *E. globulus*

Ninety metabolites were quantified and used for statistical analyses (see supplementary information available as Supplementary Data at *Tree Physiology* Online). The 90 metabolites were non-redundant (i.e., not multiple peaks per metabolite) and do not include another 40–50 low-abundance metabolites that occurred in <50% of samples. Of the 90 metabolites, 70 were positively identified (according to Metabolomics Standards Initiative criteria, Sumner et al. 2007), seven matched unknowns reported in the Golm Metabolome Database and 13 were unknowns.

The concentration of measured inorganic ions was approximately the same as the concentration of aqueous metabolites (Figure 4). The dominant inorganic ions were potassium and chloride. Nitrate, ammonium and phosphate were present at very small concentrations or below detection limits in most samples (see below). Glucose 1-P, glucose 6-P and fructose 6-P were present in low concentrations, and no other sugar phosphates were detected. The pool of aqueous metabolites was dominated by carbohydrates and organic/phenolic acids (Figure 4). The most abundant carbohydrates were sucrose, raffinose, fructose, glucose, galactinol, myo-inositol and scyllo-inositol. The most abundant organic/phenolic acids were shikimic, malic and quinic acids.

Effect of P on leaf metabolites

OPLS-DA was used to separate multivariate relationships into predictive variation (related to P treatment) and orthogonal variation (unrelated to treatment). An OPLS-DA model with one predictive and one orthogonal component gave a reasonable fit to the data ($R^2Y = 0.87$ and $Q^2 = 0.43$) and was significant (ANOVA testing of cross-validated predictive residuals, $P < 0.05$). Ten percent of variation in the OPLS-DA models was due to P treatment and 24% was orthogonal variation.

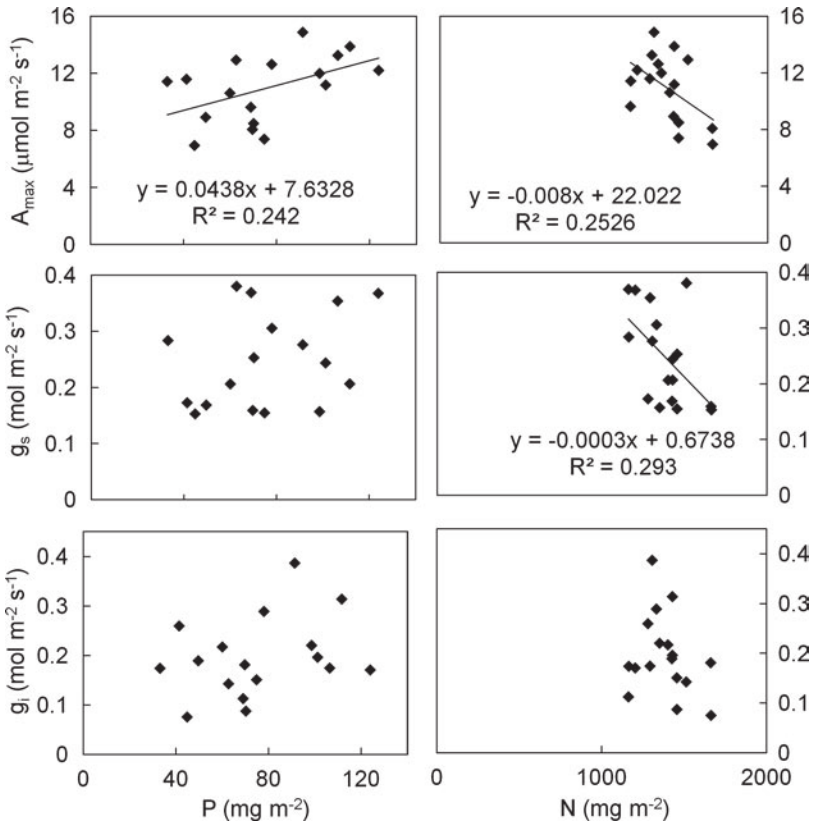

Figure 2. Relationships between photosynthetic characteristics and phosphorus content per unit area and nitrogen content per unit area of *E. globulus* seedlings grown with one of four P treatments. Gas exchange and tuneable diode laser measurements at ambient CO_2 and light saturating PAR were used to determine the rate of net photosynthesis (A_{max}), stomatal conductance to water (g_s) and internal conductance to CO_2 (g_i). Regressions are shown where significant ($P < 0.05$). Data are individual plants.

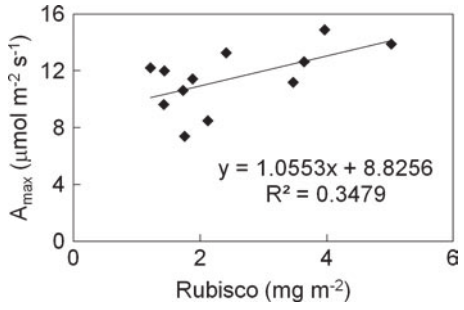

Figure 3. Relationships between the rate of net photosynthesis (A_{max}) and Rubisco content per unit area of *E. globulus* seedlings grown with one of four P treatments. Data are individual plants.

Analysis of loading plots with jack-knifed confidence intervals showed that increasing concentration of P in the nutrient solution increased amounts of 19 metabolites and decreased amounts of 13 metabolites (OPLS-DA loading ± confidence interval ≠ 0) (see supplementary information available as Supplementary Data at *Tree Physiology* Online). Visual analysis of an S-plot (Figure 5) permitted identification of those metabolites that made a large contribution to the model (*x*-axis, modelled covariation) and were reliable (*y*-axis, modelled correlation). Those metabolites strongly correlated with the OPLS-DA model and increased by P were [P], phosphate, glucose 6-P, fructose 6-P, threonic acid, threonic acid lactone, four biosynthetically related compounds (galactinol, sucrose, myo-inositol and raffinose), and Phe plus the related compounds catechin and coumaroylquinic acid. Metabolites strongly negatively associated with the OPLS-DA model were arginine, glutamine, ammonium, threonine, alanine, quinic acid, glucose, [N] and erythronic acid.

To visualize the effect of P on metabolites, metabolite concentrations were projected onto simplified biochemical pathways (Figure 6). Phosphorus supply had a large effect on the quantified P-containing metabolites: phosphate (sixfold increase from P0.0 to P0.1 treatments), glucose 6-P (threefold increase) and fructose 6-P (fourfold increase). Phosphorus supply affected four metabolites of the phenylpropanoid pathway: phenylalanine (1.5-fold increase), 5-coumaroylquinic acid (2.5-fold increase), catechin (fourfold increase), and quinic acid (twofold decrease). Increasing P supply led to small increases in galactinol and raffinose, but not the biosynthetically related sucrose and myo-inositol (cf. the OPLS-DA model). Concentrations of fructose and glucose decreased 1.5-fold with increasing P supply. Organic acids of the TCA cycle were generally unaffected by P supply. Ascorbate and aldarate metabolism were affected

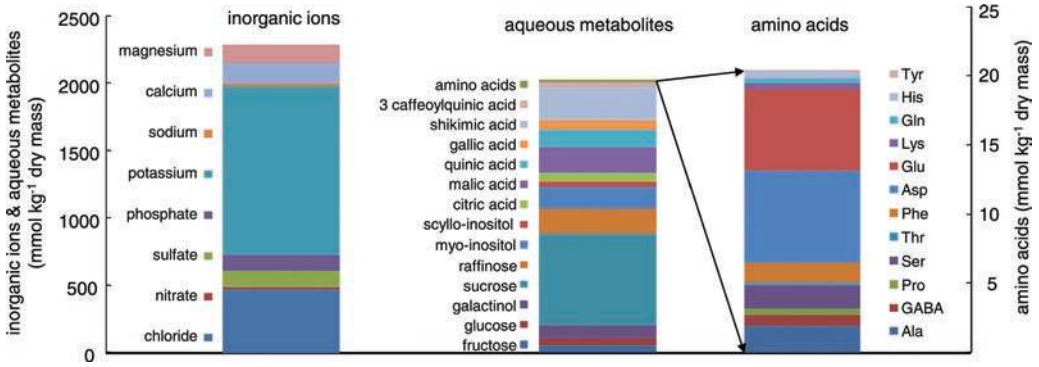

Figure 4. The profiles of inorganic ions and aqueous organic metabolites in leaves of *Eucalyptus globulus* seedlings grown with 0.1 mM P in the nutrient solution. The pool of aqueous metabolites shows only those metabolites that accounted for more than ~5% of the total pool. The expanded view of amino acids shows only those amino acids that were detected in >50% of seedlings. Note different *y*-axis scales for amino acids versus inorganic ions and total aqueous metabolites. Data are means of five replicate plants.

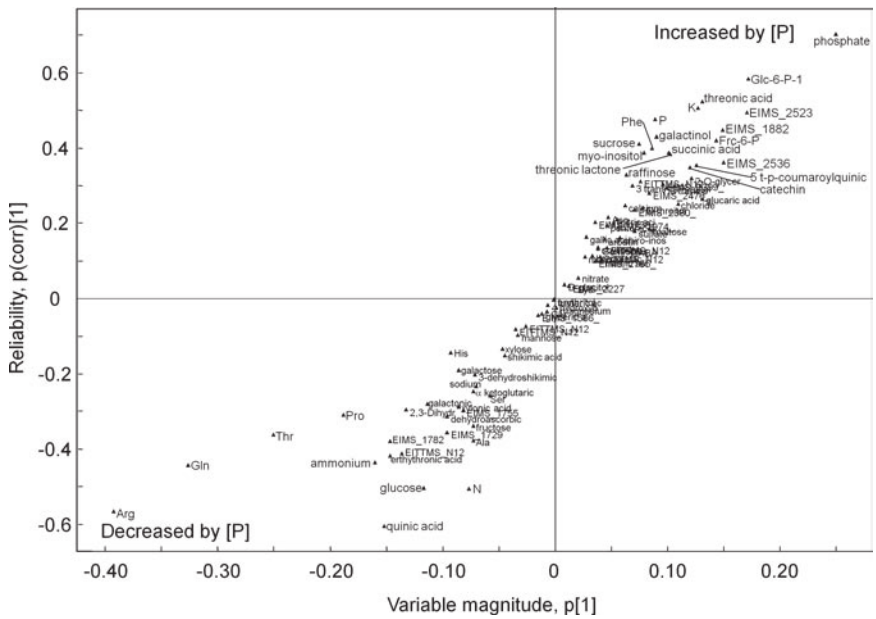

Figure 5. S-plots of an OPLS-DA model for *E. globulus* grown with four different P treatments. The *x*-axis is the modelled covariation ('magnitude'), while the *y*-axis is the loading vector of the predictive component (modelled correlation or 'reliability'). Metabolites in the upper right quadrant of S-plots are positively related to the concentration of P in nutrient solution while those in the lower left quadrant are negatively related to the concentration of P in nutrient solution. Supplementary S1 available as Supplementary Data at *Tree Physiology* Online shows loadings and Jack-knifed confidence intervals for metabolites with OPLS-DA loading ± confidence interval ≠ 0.

with increasing P supply, leading to larger concentrations of threonic acid, threonic acid lactone and threitol, and a decrease in dehydroascorbic acid. Concentrations of most amino acids were unaffected by P treatments. Notable exceptions to this were phenylalanine, which was less abundant in the P0.0 treatment than in any of the treatments with larger P supply (see above). In addition there were large decreases in arginine, glutamine and ammonium as P supply increased.

Relationships between photosynthesis and amounts of metabolites and Rubisco

Orthogonal projection to latent structures was used to develop a multivariate model for predicting A_{max} from metabolite data. The modest number of replicates meant that OPLS models were severely overfitted ($Q^2 << 0.5$ and ANOVA testing of cross-validated predictive residuals >> 0.05) unless the number of variables (metabolites and Rubisco) was reduced to <40. Variables with little predictive value were removed by successively fitting an OPLS model, deleting the five variables with smallest variable importance in the projection (VIP) and refitting the model until the model was stable and significant (based on acceptable Q^2 and ANOVA testing of cross-validated predictive residuals <0.05). The final OPLS model of 37 variables (36 metabolites + Rubisco) comprised one predictive component, was a reasonable fit to A_{max} ($R^2Y = 0.63$, $Q^2 = 0.51$, see also Figure 7) and was significant (ANOVA testing of cross-

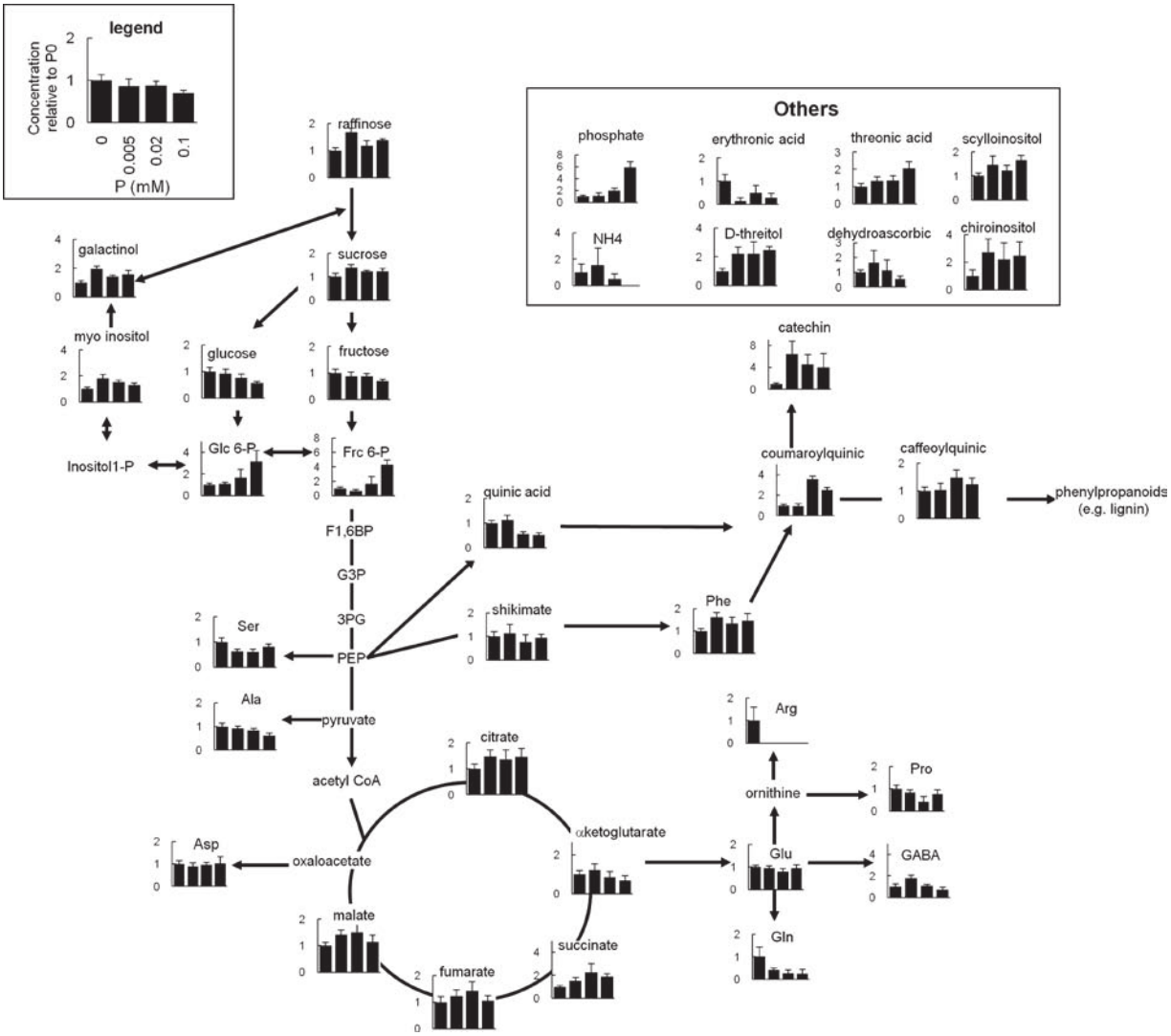

Figure 6. Mapping of relative metabolite concentrations on known pathways for leaves of *E. globulus* seedlings grown with four different P treatments (from left to right: 0, 0.005, 0.02 and 0.1 mM P). Data are normalized (to 1) of the mean response in the P0 treatment. Data are mean and standard error of five replicate plants.

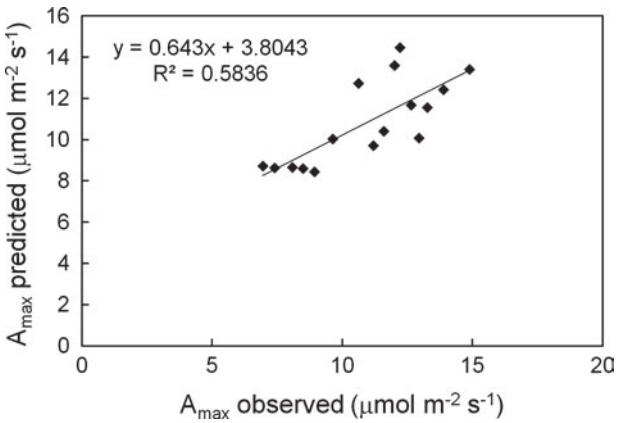

Figure 7. Correlation between the measured rate of net photosynthesis (A_{max}) and A_{max} predicted from an OPLS model. The OPLS model of 37 variables (36 metabolites + Rubisco) comprised one predictive component, was a reasonable fit to A_{max} ($R_2Y = 0.63$, $Q_2 = 0.51$) and was significant (ANOVA testing of cross-validated predictive residuals, $P = 0.009$).

validated predictive residuals, $P = 0.009$). Four metabolites (P, phosphate, fructose 6-P, and unknown with a retention index of 2523) had positive coefficients and made significant (VIP > 1) contributions to the OPLS model for A_{max} (Figure 8). Rubisco and 16 metabolites had positive coefficients, but were not significant (VIP < 1). Seven metabolites (four unknowns plus threonine, xylonic, erythronic and quinic acids) had negative coefficients and made significant (VIP > 1) contributions to the OPLS model for A_{max}.

Discussion

Growth and diffusional limitations of photosynthesis

Phosphorus supply affected processes at multiple spatial and temporal scales, viz., photosynthesis, leaf metabolites, allocation to roots versus leaves and growth (Figures 1, 2, 5 and 6).

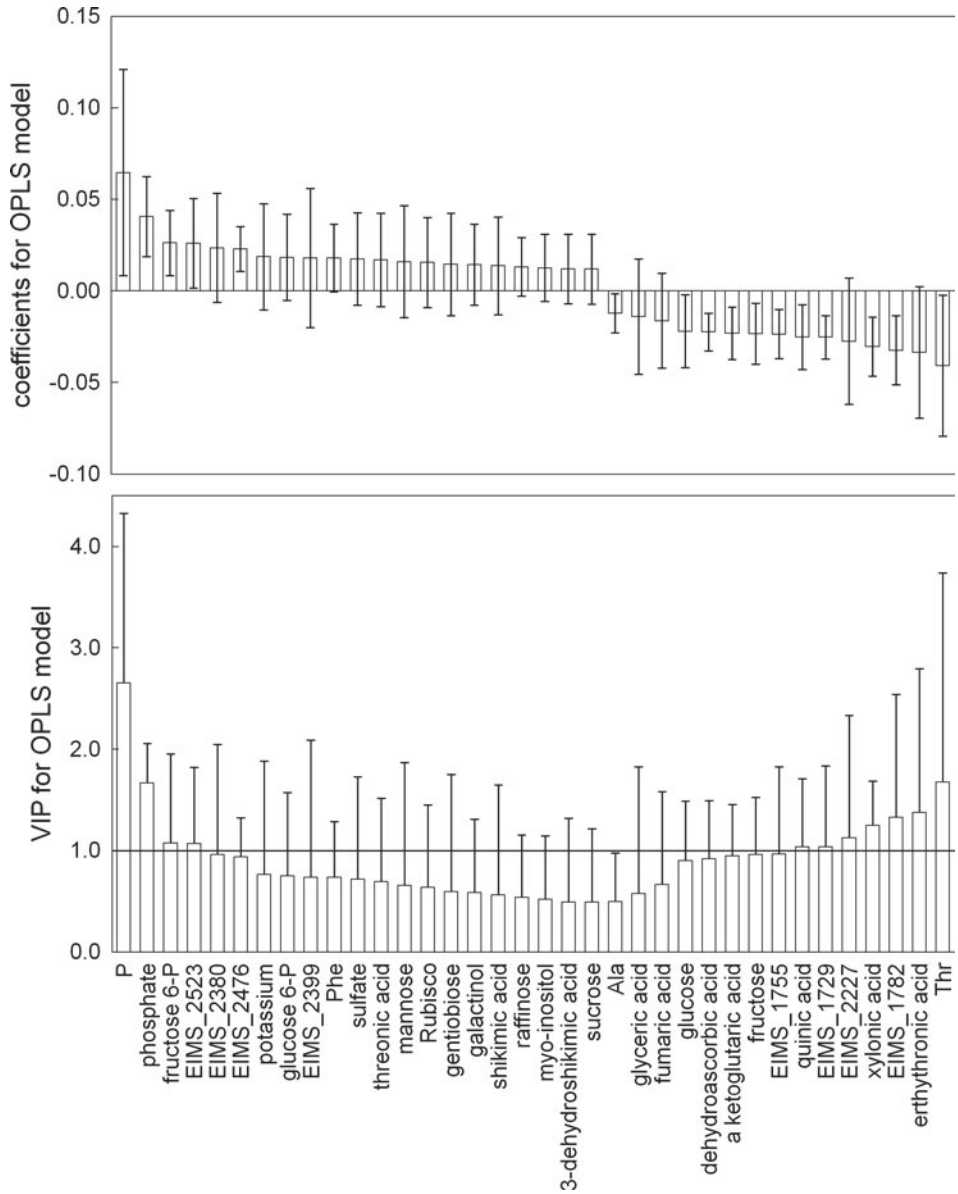

Figure 8. Coefficients and VIP for 37 variables in an OPLS model predicting the rate of net photosynthesis (A_{max}). Coefficients are for the *x*-variables Pareto scaled and centred, and the *y*-variable Pareto scaled. Variable importance to the projection indicates the importance of terms in the OPLS model with respect to A_{max} and the projection. The sum of squares of all VIP values is equal to the number of terms in the model and thus the average VIP is 1. Variables with VIP > 1 are most relevant for explaining variation in A_{max}.

Use of four nutrient solutions varying in P concentration led to leaf P concentrations (0.6–1.4 mg g^{-1}) spanning the range from deficient to adequate (Turnbull et al. 2007) and leaf N:P ratios that varied from 12 g g^{-1} in the P0.1 treatment (indicative of adequate P, Koerselman and Meuleman 1996) to 26 g g^{-1} in treatments with a smaller P supply (indicative of P limitation, Koerselman and Meuleman 1996). Leaf N concentrations were adequate for *E. globulus*, and thus effects observed in this study can be attributed to P concentrations varying from deficient to adequate.

There was no evidence that stomatal (g_s) or internal conductance (g_i) contributed to the effect of P on photosynthesis. Phosphorus supply did not affect the drawdown in CO_2 from atmosphere to sub-stomatal cavities ($C_a - C_i = A_{max}/g_{sCO_2}$) or sub-stomatal cavities to chloroplasts ($C_i - C_c = A_{max}/g_i$). This contrasts with some studies reporting that reduced g_s and C_i contributed to reductions in photosynthesis in P-limited plants (e.g., Kirschbaum and Tompkins 1990, Lewis et al. 1994). However, data are consistent with the only other study of responses of g_i to P (Bown et al. 2009). The authors found that in *P. radiata* there was no effect of P supply on C_i–C_c or relative limitations due to g_i (Bown et al. 2009). In the case of *E. globulus* we may have extra confidence in our instantaneous measurements of g_i and g_s because the absence of treatment

differences in $\delta^{13}C$ of leaves (Table 1) indicates that C_c (integrated over the time C in the leaf was fixed) did not differ between treatments (Farquhar et al. 1989). The consistency of results from the gymnosperm *P. radiata* and angiosperm *E. globulus* hints at a general response between P and g_i; however, additional studies with other species are required to establish the general relationship between P and g_i.

Metabolite profiles and biochemical limitations of photosynthesis

Biochemical limitations played the major role in the response of photosynthesis to P supply, which was not unexpected given the strong effect of P supply on metabolite profiles. Previous studies reported that P deficiency reduces V_{cmax}, J and TPU (Lewis et al. 1994, Loustau et al. 1999, Niinemets et al. 1999) but such data are hard to interpret because in these previous studies 'biochemical' parameters were determined on the basis of C_i and thus contain information pertaining to C_i–C_c (i.e., g_i) as well as biochemistry (Warren 2008). However, this may not be a major problem given that V_{cmax}, J and TPU determined on the basis of C_c were also positively related to P supply (Table 1). Phosphorus supply affected all three biochemical parameters of photosynthesis (i.e., V_{cmax}, J and TPU), but analysis of CO_2 responses and C_c showed that V_{cmax} was the sole limitation of A_{max}. One explanation for the single-handed limitation of A_{max} by V_{cmax} is that TPU limitation is a short-term effect and in the long term (days to weeks) the limitation shifts from TPU to V_{cmax} due to large reductions in V_{cmax} (Lewis et al. 1994, Campbell and Sage 2006).

Metabolite profiling and quantification of Rubisco provided some insights into the biochemical basis for the effect of P on A_{max}, V_{cmax}, J and TPU. There was a trend for P-deficient seedlings to contain less Rubisco than P-replete seedlings, but this was not statistically significant (Table 1) and did not make a significant contribution to an OPLS model for predicting A_{max} (Figures 7 and 8). Better predictors of A_{max} were P-containing compounds (P, phosphate, fructose 6-P), which is not surprising given that photosynthesis and much of primary metabolism is dependent on pools of phosphate and phosphorylated intermediates such as fructose 6-P (Walker and Robinson 1978). It is notable that the decreases in phosphate (sixfold decrease), glucose 6-P (threefold decrease) and fructose 6-P (threefold decrease) due to P deficiency were larger than the decrease in photosynthesis. Hence, reductions in phosphate and phosphorylated intermediates do not necessarily have a severe (or proportional) impact on C metabolism (cf. Huang et al. 2008). Instead, P deficiency leads to greater efficiency with smaller pools of phosphate and phosphorylated intermediates turning over more rapidly. For the metabolites negatively related to A_{max} (threonine; quinic, xylonic and erythronic acids), it is difficult to conceive a direct role in photosynthesis and thus their correlation with A_{max} most likely reflects an underlying correlation with P supply rather than photosynthesis.

Phosphorous deficiency had a negligible effect on carbohydrates and TCA cycle organic acids, which is at odds with the large reductions in A_{max}, P-containing metabolites, and other studies showing large effects of P on carbohydrates and TCA cycle organic acids (Pieters et al. 2001, Hernandez et al. 2007, Huang et al. 2008). Nevertheless, some studies have reported similarly small effects of P supply on carbohydrates (Nanamori et al. 2004, Tissue and Lewis 2010), and this difference between studies is probably partly due to species differences (e.g., Nanamori et al. 2004) and partly due to the duration of P stress. When stress is imposed over a period of several months, as in the present study and some others (e.g., Tissue and Lewis 2010), there is enough time for C metabolism to balance with rates of photosynthesis and growth and there are minimal effects on pools of carbohydrates (i.e., there is a functional homeostasis).

The effect of P supply on most amino acids was small or non-significant, which is consistent with the general absence of effects on carbohydrates and TCA cycle organic acids. Notable exceptions were arginine and glutamine, which increased dramatically under P deficiency (Figure 6), as has also been observed in response to high N supply, low P supply or an imbalance between N and other elements (Durzan and Steward 1967, Huang et al. 2008). There are at least two explanations for the accumulation of N-rich amino acids under P deficiency. It could be that N-rich amino acids (e.g., arginine with 4 N and glutamine with 2 N) are a good way to store N when supply exceeds demand, for example, if growth is limited by another nutrient such as P. An alternative explanation is that accumulation of arginine and glutamine is a response to avoid ammonium toxicity—a supposition supported by the larger concentrations of ammonium under P deficiency (Figure 6) (Huang et al. 2008). It is suggested that P deficiency leads to a shortage of C skeletons, so proteins and amino acids are deaminated for use in C metabolism—with concomitant production of ammonium, which must be detoxified (Huang et al. 2008). There are insufficient data to distinguish between these possibilities, but the ammonium detoxification scenario seems unlikely for two reasons. First, there was little evidence for a strong shortage of C skeletons with only small changes in amounts of most amino acids, sugars and organic acids of the TCA cycle. Second, *E. globulus* is not very sensitive to ammonium and it is, in fact, one of the major forms of N taken up by *E. globulus* and other *Eucalyptus* species (Warren 2009).

Up-regulation of the phenylpropanoid pathway and increased amounts of anthocyanins and phenols are common responses to deficiencies of P and other nutrients such as N (e.g., Juszczuk et al. 2004, Close et al. 2007). However, in seedlings of *E. globulus*, P deficiency decreased the amounts of phenylalanine, coumaroylquinic acid and catechin (Figures 5 and 6).

This might be because P deficiency increases the rate of lignification (Uhde-Stone et al. 2003) and this draws down pools of phenylalanine, coumaroylquinic acid and catechin. An alternative explanation is that the phenylpropanoid pathway also responds to N (e.g., Close et al. 2007), and thus low phenylalanine, coumaroylquinic acid and catechin in the P0.0 treatment may have been because seedlings in the P0.0 treatment had higher N concentrations than the other treatments.

Conclusions

Gas exchange and GC-MS metabolite profiling indicated that P affects processes operating at multiple spatial and temporal scales, viz., photosynthesis, leaf metabolites, allocation to roots versus leaves and growth. P deficiency reduced photosynthesis by ~50% and this was primarily due to biochemical factors (e.g., as indicated by the parameter V_{cmax} and correlations with pools of phosphate and hexose phosphates). Decreases in phosphate (sixfold decrease), glucose 6-P (threefold decrease) and fructose 6-P (fourfold decrease) were larger than the 50% decrease in photosynthesis, indicating that P deficiency increases the 'efficiency' with which phosphate and sugar phosphates are used in photosynthesis—most likely due to smaller pools with faster turnover. The drawdown in CO_2 concentration from atmosphere to sub-stomatal cavities (C_a–C_i) and chloroplasts (C_i–C_c) was not the cause of P-induced changes in photosynthesis. Phosphorus deficiency affected amounts of around one-third of metabolites, but the effect size was generally smaller than seen in other studies. The effects of P deficiency on carbohydrates, TCA cycle organic acids and most amino acids were small, particularly in comparison with experiments with more rapid and shorter-term treatments. The small response of *E. globulus* compared with other species may reflect inherent species differences, or could be because the 2.5-month duration of the P treatment provided sufficient time for a functional homeostasis among C metabolism (glycolysis, TCA and pentose P cycles), rates of photosynthesis and growth.

Acknowledgments

Dr Maria Taranto is warmly thanked for assisting with preparation of samples. I acknowledge the technical expertise of Sam Ruggeri in manufacturing the custom leaf cuvette for the LI-6400.

Funding

Australian Research Council (DP0662752, LE0882935).

Supplementary data

Supplementary data for this article are available at *Tree Physiology* Online.

References

Barbour, M.M., G.D. Farquhar, D.T. Hanson, C.P. Bickford, H. Powers and N.G. McDowell. 2007. A new measurement technique reveals temporal variation in delta O-18 of leaf-respired CO_2. Plant, Cell Environ. 30:456–468.

Bernacchi, C.J., A.R. Portis, H. Nakano, S. von Caemmerer and S.P. Long. 2002. Temperature response of mesophyll conductance. Implications for the determination of Rubisco enzyme kinetics and for limitations to photosynthesis in vivo. Plant Physiol. 130:1992–1998.

Bickford, C.P., N.G. McDowell, E.B. Erhardt and D.T. Hanson. 2009. High-frequency field measurements of diurnal carbon isotope discrimination and internal conductance in a semi-arid species, *Juniperus monosperma*. Plant, Cell Environ. 32:796–810.

Bown, H.E., M.S. Watt, E.G. Mason, P.W. Clinton and D. Whitehead. 2009. The influence of nitrogen and phosphorus supply and genotype on mesophyll conductance limitations to photosynthesis in *Pinus radiata*. Tree Physiol. 29:1143–1151.

Bylesjö, M., M. Rantalainen, O. Cloarec, J.K. Nicholson, E. Holmes and J. Trygg. 2006. OPLS discriminant analysis: combining the strengths of PLS-DA and SIMCA classification. J. Chemometrics 20:341–351.

Campbell, C.D. and R.F. Sage. 2006. Interactions between the effects of atmospheric CO_2 content and P nutrition on photosynthesis in white lupin (*Lupinus albus* L.). Plant, Cell Environ. 29:844–853.

Chabot, B.F. and D.J. Hicks. 1982. The ecology of leaf life spans. Annu. Rev. Ecol. Syst. 13:229–259.

Close, D.C., C. McArthur, A.E. Hagerman, N.W. Davies and C.L. Beadle. 2007. Phenolic acclimation to ultraviolet-A irradiation in *Eucalyptus nitens* seedlings raised across a nutrient environment gradient. Photosynthetica 45:36–42.

Durzan, D.J. and F.C. Steward. 1967. Nitrogen metabolism of *Picea glauca* (Moench) Voss and *Pinus banksiana* Lamb. as influenced by mineral nutrition. Can. J. Bot. 45:695–710.

Evans, J.R., T.D. Sharkey, J.A. Berry and G.D. Farquhar. 1986. Carbon isotope discrimination measured concurrently with gas-exchange to investigate CO_2 diffusion in leaves of higher-plants. Aust. J. Plant Physiol. 13:281–292.

Farquhar, G.D., S. von Caemmerer and J.A. Berry. 1980. A biochemical model of photosynthetic CO_2 assimilation in leaves of C_3 species. Planta 149:78–90.

Farquhar, G.D., J.R. Ehleringer and K.T. Hubick. 1989. Carbon isotope discrimination and photosynthesis. Annu. Rev. Plant Physiol. Plant Mol. Biol. 40:503–537.

Feller, I.C. 1996. Effects of nutrient enrichment on leaf anatomy of dwarf *Rhizophora mangle* L (Red mangrove). Biotropica 28:13–22.

Hernandez, G., M. Ramirez, O. Valdes-Lopez et al. 2007. Phosphorus stress in common bean: root transcript and metabolic responses. Plant Physiol. 144:752–767.

Huang, C.Y., U. Roessner, I. Eickmeier, Y. Genc, D.L. Callahan, N. Shirley, P. Langridge and A. Bacic. 2008. Metabolite profiling reveals distinct changes in carbon and nitrogen metabolism in phosphate-deficient barley plants (*Hordeum vulgare* L.). Plant Cell Physiol. 49:691–703.

Juszczuk, I.M., A. Wiktorowska, E. Malusa and A.M. Rychter. 2004. Changes in the concentration of phenolic compounds and exudation induced by phosphate deficiency in bean plants (*Phaseolus vulgaris* L.). Plant Soil 267:41–49.

Kirschbaum, M.U.F. and D. Tompkins. 1990. Photosynthetic responses to phosphorus-nutrition in *Eucalyptus grandis* seedlings. Aust. J. Plant Physiol. 17:527–535.

Koerselman, W. and A.F.M. Meuleman. 1996. The vegetation N:P ratio: a new tool to detect the nature of nutrient limitation. J. Appl. Ecol. 33:1441–1450.

Kusano, M., A. Fukushima, H. Redestig and K. Saito. 2011. Metabolomic approaches toward understanding nitrogen metabolism in plants. J. Exp. Bot. 62:1439–1453.

Lanigan, G., N. Betson, H. Griffiths and U. Seibt. 2009. Carbon isotope fractionation during photorespiration and carboxylation in *Senecio*. Plant Physiol. 148:2013–2020.

Lewis, J.D., K.L. Griffin, R.B. Thomas and B.R. Strain. 1994. Phosphorus supply affects the photosynthetic capacity of loblolly-pine grown in elevated carbon-dioxide. Tree Physiol. 14:1229–1244.

Lisec, J., N. Schauer, J. Kopka, L. Willmitzer and A.R. Fernie. 2006. Gas chromatography mass spectrometry-based metabolite profiling in plants. Nat Prot. 1:387–396.

Loustau, D., M. Ben Brahim, J.P. Gaudillere and E. Dreyer. 1999. Photosynthetic responses to phosphorus nutrition in two-year-old maritime pine seedlings. Tree Physiol. 19:707–715.

Millard, P. 1996. Ecophysiology of the internal cycling of nitrogen for tree growth. Z Pflanzenernahrung Bodenkunde 159:1–10.

Murphy, J. and J.P. Riley. 1962. A modified single solution method for the determination of phosphate in natural waters. Anal. Chim. Acta 27:31–36.

Nanamori, M., T. Shinano, J. Wasaki, T. Yamamura, I.M. Rao and M. Osaki. 2004. Low phosphorus tolerance mechanisms: phosphorus recycling and photosynthate partitioning in the tropical forage grass, *Brachiaria* hybrid cultivar mulato compared with rice. Plant Cell Physiol. 45:460–469.

Niinemets, U., J.D. Tenhunen, N.R. Canta, M.M. Chaves, T. Faria, J.S. Pereira and J.F. Reynolds. 1999. Interactive effects of nitrogen and phosphorus on the acclimation potential of foliage photosynthetic properties of cork oak, *Quercus suber*, to elevated atmospheric CO_2 concentrations. Glob. Change Biol. 5:455–470.

Okazaki, K., N. Oka, T. Shinano, M. Osaki and M. Takebe. 2008. Differences in the metabolite profiles of spinach (Spinacia oleracea L.) leaf in different concentrations of nitrate in the culture solution. Plant Cell Physiol. 49:170–177.

Pieters, A.J., M.J. Paul and D.W. Lawlor. 2001. Low sink demand limits photosynthesis under P-i deficiency. J. Exp. Bot. 52:1083–1091.

Sardans, J., J. Penuelas and F. Roda. 2006. Plasticity of leaf morphological traits, leaf nutrient content, and water capture in the Mediterranean evergreen oak *Quercus ilex* subsp *ballota* in response to fertilization and changes in competitive conditions. Ecoscience 13:258–270.

Schauer, N., D. Steinhauser, S. Strelkov et al. 2005. GC-MS libraries for the rapid identification of metabolites in complex biological samples. FEBS Lett. 579:1332–1337.

Sumner, L.W., A. Amberg, D. Barrett et al. 2007. Proposed minimum reporting standards for chemical analysis. Metabolomics 3:211–221.

Tazoe, Y., S. Von Caemmerer, M.R. Badger and J.R. Evans. 2009. Light and CO_2 do not affect the mesophyll conductance to CO_2 diffusion in wheat leaves. J. Exp. Bot. 60:2291–2301.

Terashima, I., Y.T. Hanba, Y. Tazoe, P. Vyas and S. Yano. 2006. Irradiance and phenotype: comparative eco-development of sun and shade leaves in relation to photosynthetic CO_2 diffusion. J. Exp. Bot. 57:343–354.

Tissue, D.T. and J.D. Lewis. 2010. Photosynthetic responses of cottonwood seedlings grown in glacial through atmospheric [CO_2] vary with phosphorus supply. Tree Physiol. 30:1361–1372.

Tschoep, H., Y. Gibon, P. Carillo, P. Armengaud, M. Szecowka, A. Nunes-Nesi, A.R. Fernie, K. Koehl and M. Stitt. 2009. Adjustment of growth and central metabolism to a mild but sustained nitrogen-limitation in Arabidopsis. Plant, Cell Environ. 32:300–318.

Turnbull, T.L., C.R. Warren and M.A. Adams. 2007. Novel mannose-sequestration technique reveals variation in subcellular orthophosphate pools do not explain the effects of phosphorus nutrition on photosynthesis in *Eucalyptus globulus* seedlings. New Phytol. 176:849–861.

Uhde-Stone, C., K.E. Zinn, M. Ramirez-Yanez, A.G. Li, C.P. Vance and D.L. Allan. 2003. Nylon filter arrays reveal differential gene expression in proteoid roots of white lupin in response to phosphorus deficiency. Plant Physiol. 131:1064–1079.

Vapaavuori, E.M., A.H. Vuorinen, P.J. Aphalo and H. Smolander. 1995. Relationships between net photosynthesis and nitrogen in Scots pine: seasonal variation in seedlings and shoots. Plant Soil 168/169:263–270.

Walker, D.A. and S.P. Robinson. 1978. Chloroplast and cell. A contemporary view of photosynthetic carbon assimilation. Ber. Deut. Bot. Ges. 91:513–526.

Warren, C.R. 2008. Stand aside stomata, another actor deserves centre stage: the forgotten role of the internal conductance to CO_2 transfer. J. Exp. Bot. 59:1475–1487.

Warren, C.R. 2009. Uptake of inorganic and amino acid N from soil by the trees *Eucalyptus regnans* and *Eucalyptus pauciflora*. Tree Physiol. 29:401–409.

Warren, C.R. and M.A. Adams. 2002. Phosphorus affects growth and partitioning of nitrogen to Rubisco in *Pinus pinaster*. Tree Physiol. 22:11–19.

Warren, C.R. and M.A. Adams. 2004*a*. Capillary electrophoresis of the major anions and cations in leaf extracts of woody species. Phytochem. Anal. 15:407–413.

Warren, C.R. and M.A. Adams. 2004b. Evergreen trees do not maximize instantaneous photosynthesis. Trends Plant Sci. 9:270–274.

Warren, C.R., M.A. Adams and Z.L. Chen. 2000. Is photosynthesis related to concentrations of nitrogen and Rubisco in leaves of Australian native plants? Aust. J. Plant Physiol. 27:407–416.

Warren, C.R., I. Aranda and F.J. Cano. 2011. Metabolomics demonstrates divergent responses of two *Eucalyptus* species to water stress. Metabolomics doi: 10.1007/s11306-011-0299-y.

Wingate, L., U. Seibt, J.B. Moncrieff, P.G. Jarvis and J. Lloyd. 2007. Variations in C-13 discrimination during CO_2 exchange by *Picea sitchensis* branches in the field. Plant, Cell Environ. 30:600–616.